Stabilization of Desired Flow Regimes in Pipelines

E.Storkaas, S. Skogestad* and V. Alstad

Department of Chemical Engineering

Norwegian University of Science and Technology, Trondheim, Norway

November 2, 2001 💬

1 Abstract

Elimination of slugging by changing the design or the operating point (e.g. increasing the pressure) has been suggested by many authors. The objective for them was to get to an operating point where the desired flow regime is (open-loop) stable. In this paper the objective is to stabilize the unstable (optimal) operating point using feedback control.

A simple two-phase flow model is used for analysis and controller design. The model captures the main dynamics of severe slugging, and is first order continuous, thus suited for linear analysis and controller design. We have shown that a system exhibiting severe slugging is a Hopf bifurcation with the choke valve position as free variable.

The pressure sensor used as measurement for control should be placed in the lower part of the system. With the pressure sensor located in the riser, RHP-zeros close to the imaginary axis limits the bandwidth of the control system, making stabilization of the system difficult.

The task of eliminating severe slugging in pipelines consists of two sub-problems;

1. Breaking the limit cycle and bringing the system to the desired operating point

2. Stabilize the system at the desired operating point

In this work we show that it is possible to break the limit cycle manually by closing the choke valve and then bring the system to its desired closed-loop stable operating point using a simple PI-controller.

---

*email: skoge@chembio.ntnu.no

2 Introduction

Stabilization of desired fluid flow regimes offers challenges of immense potential value. The opportunities for control engineers in this field are very large, because most fluid flow experts tend to be "feedforward thinkers" with only limited insight into the potential benefits of feedback control. They tend to believe that the stability regions of a given steady-state flow pattern is fixed by nature. However, these are open-loop stability regions, and with feedback control one may change these boundaries.

The most well-known example is probably the transition from laminar to turbulent flow in single phase pipelines which is known to occur at a Reynolds-number of about 2300. However, it is well known that by carefully increasing the flow rate one may achieve laminar flow at much larger Re-numbers, but that in this case a small knock at the pipeline will immediately change the flow to turbulent. Some attempts have been made in applying control to this problem (e.g. see Bewley (2000) for a survey), but the short time and length scales make practical applications difficult.

Another unstable flow phenomenon occurs in multi-phase pipelines, where pressure-flow fluctuations known as slug-flow can be induced both by velocity difference between the gas and liquid phase (hydrodynamic slugging) and by the pipe geometry (severe slugging, terrain slugging, riser induced slugging). The latter severe slugging phenomenon occurs at a time and length scale that makes control a viable option. In many cases severe slugging induced by the terrain on the seabed or by the vertical distance to the platform is a major problem for production, as it leads to large load disturbances for the inlet separator causing compressor trip or flooding of the separator.

Unstable flow in multi-phase transport systems can usually be avoided by either changing the operating point or redesigning the system. A description of different approaches to avoid unstable flow regimes can be found in Sarica and Tengesdal (2000). Up until very recently, the standard method for avoiding this problem has been to change the operating point by closing the choke-valve opening. However, the optimal operating point for many systems is inside the unstable region, and increasing the downstream pressure results in economic loss.

In many, if not most, cases the problems with unstable flow regimes occurs as the oilfields get older and the gas-to-oil ratio and water cut increases. Initially stable transport systems can in many cases experience severe stability problems after a few years of production. Since these transport systems are highly capital cost intensive, retrofitting or rebuilding these systems is rarely an option. Thus, a effective way to stabilize unstable flow regimes is clearly the best way to handle a multiphase transport system gone unstable.

The use of feedback control to avoid severe slugging was proposed and applied on a test rig by Hedne and Linga (1990). Later independent studies, including simulations and actual full-scale implementations, are reported by

Henriot et al. (1999) and Havre et al. (2000). The two-phase simulations were performed using the industrial simulators TACITE and OLGA, respectively, but these were essentially used as "black box" simulators to test the proposed control strategies. None of the control systems are based on an first principles dynamic model and subsequent analysis and controller design. It is our view that in order to achieve robust stabilization for a wide range of cases, a controller based on a simple model describing the dominant dynamic characteristics of the system is needed.

3   Severe Slugging Phenomenon

The cyclic behavior of severe slugging is illustrated schematically in figure 1.
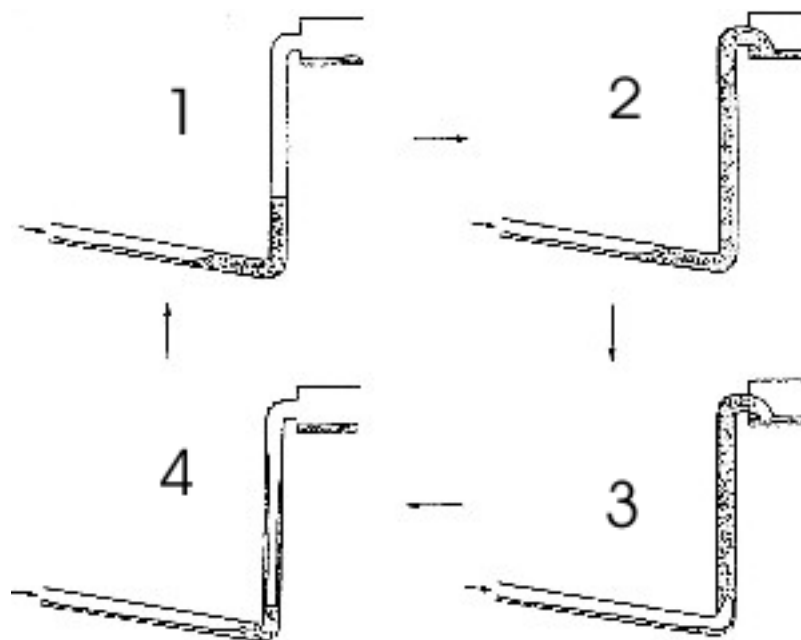
Figure 1: Graphic illustration of a slug cycle

It can be broken down into four parts. First, the liquid accumulates in the low point. A prerequisite for severe slugging to occur is that the gas and liquid velocity is low enough to allow for this accumulation. The liquid blocks the gas flow, and a continuous liquid slug is formed in the riser. As long as the rate of pressure increase upstream the slug is lower than the rate of increase of the hydrostatic head of the liquid in the riser, the slug will continue to grow(step 2).

When the pressure behind the slug overcomes the hydrostatic head of the liquid column, the gas will start penetrating the liquid in the riser and push the liquid out (step 3). Since this is accompanied with a pressure drop, the

gas will expand and further increase the velocities in the riser. After the majority of the liquid and the gas has left the riser, the velocity of the gas is no longer high enough to pull the liquid upwards. The liquid will start flowing back down the riser (step 4) and the accumulation of liquid starts again.

A more detailed description of the severe slugging phenomenon can be found in Taitel (1986).

4 Model Description

Two types of one-dimensional models are commonly used when modeling multiphase flow; *the drift flux model*, with mass balances for each phase and a combined momentum balance, and *the two-fluid model*, with separate mass and momentum balances for each phase. For the drift flux type model, one also needs algebraic equations relating the velocities in the different phases.

In this work we used a two-fluid model for a two phase system. The conservation equations for mass and momentum then consists of four Partial Differential Equations(PDEs):

$$\frac{\partial}{\partial t}\left(\alpha_L \rho_L\right) + \frac{1}{A}\frac{\partial}{\partial x}\left(\alpha_L \rho_L u_L A\right) = 0$$

$$\frac{\partial}{\partial t}\left(\alpha_G \rho_G\right) + \frac{1}{A}\frac{\partial}{\partial x}\left(\alpha_G \rho_G u_G A\right) = 0$$

$$\frac{\partial}{\partial t}\left(\alpha_L \rho_L u_L\right) + \frac{1}{A}\frac{\partial}{\partial x}\left(\alpha_L \rho_L u_L^2 A\right) = -\frac{\alpha_L}{A}\frac{\partial}{\partial x}\left(\alpha_L A\right) + \alpha_L \rho_L g_x - \frac{S_{Lw}}{A}\tau_{Lw} + \frac{S_i}{A}\tau_i$$

$$\frac{\partial}{\partial t}\left(\alpha_G \rho_G u_G\right) + \frac{1}{A}\frac{\partial}{\partial x}\left(\alpha_G \rho_G u_G^2 A\right) = -\frac{\alpha_G}{A}\frac{\partial}{\partial x}\left(\alpha_G A\right) + \alpha_G \rho_G g_x - \frac{S_{Gw}}{A}\tau_{Gw} + \frac{S_i}{A}\tau_i$$

Here we have assumed the following

- Constant liquid density ρ_L

- Constant pressure over a pipe cross-section, implying equal pressure in both phases

- No mass transfer between the phases

- No liquid droplet field in the gas

- Isothermal conditions

- Ideal gas equation of state

Algebraic relations for friction and relations between wetted perimeter and phase fraction are needed. These, and other details about the model are given in the appendix.

This will give four states ($\alpha_L \rho_L$, $\alpha_G \rho_G$, $\alpha_L \rho_L u_L$ and $\alpha_L \rho_L u_L$), which together with the summation equation for the phase fractions $\alpha_L + \alpha_G = 1$ gives the phase fractions, gas density and both velocities.

Horizontal and inclined flow is fundamentally different due to the effect of gravity. This model is based on stratified flow for the horizontal pipe sections, and annular or bubbly flow for inclined pipe sections. This does not introduce discontinuities, as this switch is only dependent on geometry.

For inclined flow, the possibility for annular and bubbly flow is included. It is assumed that the same algebraic relation between phase densities, velocities and friction is valid for all flow regimes, both horizontal and inclined. The expression for the wetted parameter is the only difference between the regimes. For bubble flow in inclined pipes, the wetted perimeter is computed based on an average bubble diameter. For annular flow, the wetted perimeter is that of a gas core in a body of liquid. The transition between the regimes is modeled using a sinusoidal weighting function (weight 0-1), and is assumed only to be a function of phase fraction. This ensures a smooth transition.

The choke valve is modeled using the model of Sachdeva et al. (1986)

The model is implemented in MatLab.

4.1 Discretization of the PDEs

In order to solve the system of PDEs, we discretize in space and solve the resulting set of Ordinary Differential Equations (ODEs). A staggered grid approach is used, since this is required for numeric stability of the solution with standard ODE solvers (e.g. MatLab). The spatial derivatives are computed using a backward difference scheme (Patankar, 1980). Since the direction of the flow can change in this system, care has to be taken when allocating data to the ODEs. For forward flow, the data for the spatial derivatives is collected upstreams the control volume, when the flow reverses, the data is collected downstream.

4.2 Dealing with the extremes

Due to the one-dimensional nature of the model and the simplifying assumptions made, dealing with close to one-phase conditions is difficult. When the liquid fraction approaches one, the gas velocity will increase disproportionately, since the wetted perimeter of the gas, on which friction is effective, diminishes. In the real situation, under these condition the gas will be transported as bubbles in the liquid, and the friction will be significant. Also, numerical problems arise, as the ODEs will be close to "0=0" type, making

5

them sensitive to numerical noise and unphysical solutions(such as negative phase fractions)

To avoid these problems, an artificial friction term is added to the momentum balances. This term is exponential in phase fraction, linear in velocity and effective only over a narrow range of phase fractions close to the extreme values. For phase k:

$$F_k = -10000 \cdot v_k \cdot e^{5-500*\alpha_k}$$

This term effectively prevents the acceleration of the minor phase by penalizing its velocity in the momentum balance. At the same time it prevents a phase from disappearing from a control volume, by forcing the velocity of the last amounts of that phase to be zero.

4.3 Dealing with different flow regimes

Multiphase flow may change between different flow regimes. Flow regime maps, showing the stability region of the various flow patterns as function of liquid and gas velocity, have been developed based on experimental data.Baker (1954) was one of the first to investigate the stability of the different flow regimes, the resulting map for horizontal flow of oil and gas is shown in figure 2. The parameters used on the axis are
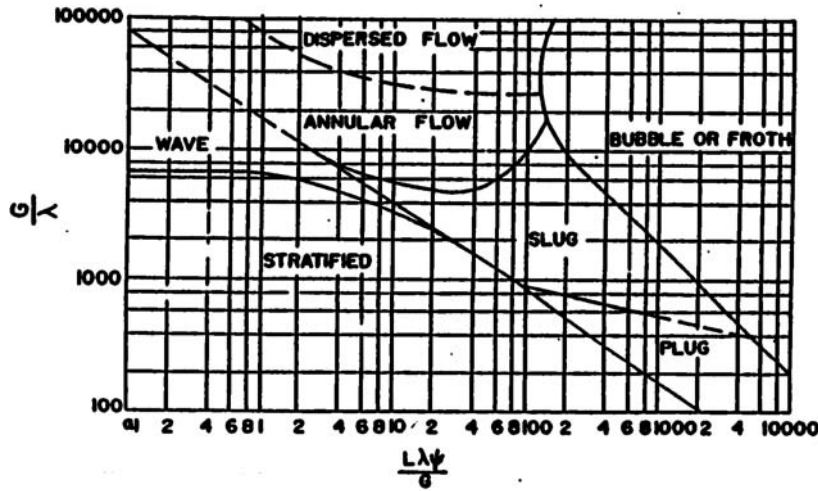
Figure 2: Flow regime map for horizontal flow of oil and gas

$$\gamma = \left[\left(\frac{\rho_G}{0.075} \right) \left(\frac{\rho_L}{62.3} \right) \right]^{0.5}, \psi = \frac{73}{\sigma} \left[\mu_L \left(\frac{62.3}{\rho_L} \right)^2 \right]^{1/3}$$

More recent work can be found in Schmidt et al. (1979). Friction, phase distribution and other system properties which depends on flow regimes are

6

computed either by algebraic correlations or interpolated from experimental data based on the predicted flow regime. Commercial multiphase flow simulators uses flow regime maps and the experimental data behind these maps to determine the flow regime and the suitable correlations for the problem at hand. However, the flow regime maps are based on *open loop* experimental data. In this work, where we are concerned with the operating in open-loop unstable operating points, the maps do not apply. Because of this, we do not use flow regime dependent correlations (except for the possibility for annular and bubbly flow in the riser, where we only consider this change to be a function of phase fraction)

Another point to be made is that incorporating flow regime dependent algebraic correlations based on open loop data will result in a discontinuous model. Linearization and succeeding analysis of such a model can give errors due to the discontinuities. An effort has been made to avoid these discontinuities.

5   Case description

In order to study the dominant characteristics of the problem, a simple case is studied. The geometry is shown in figure 3. A feed of 0.937 kg/sec of liquid and 0.063 kg/sec of gas enters into the system. Downstreams the choke valve, there is a constant pressure of 20 bar.
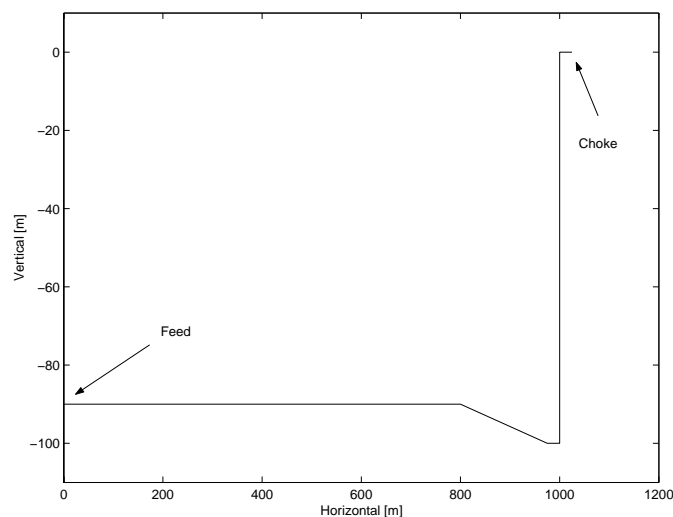
Figure 3: Geometry for the test case
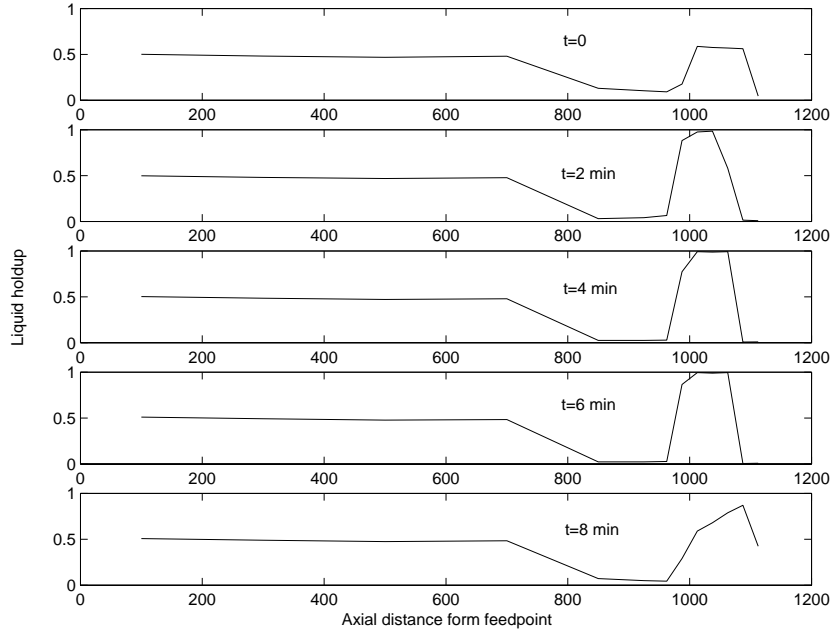
Figure 4: Liquid holdup profile through a slug cycle

6   Simulations without feedback control

With a valve opening of 0.5 the system exhibits severe slugging. The liquid
holdup profile through the slug cycle is shown in figure 4. Pressure in the
horizontal pipe section is shown as a function of time in figure 5.

As can be seen from figures 4 and 5, the liquid blocks the pipe at the low
point, and the pressure starts to rise upstreams from the blockage. As the
pressure reaches its maximum, the gas penetrates the liquid column in the
riser and pushes a majority of the liquid out of the system. This is associated
with a pressure drop and succeeding drop in the gas velocity. The gas can
no longer bring the liquid up the riser, the liquid falls back down the riser
and the cycle starts over.

Mathematically, this cyclic behavior is called a limit cycle. As will be
evident below, the reason for this is a Hopf bifurcation in the model when
considering the valve position as an independent variable. The task at hand
for control is to somehow break the limit cycle and operate at the unstable,
stationary point which exists inside the cycle. For control, we want to use
the choke valve as an actuator, and a pressure measurement as input to the
controller. The optimal location for the pressure transmitter is examined
below.

8
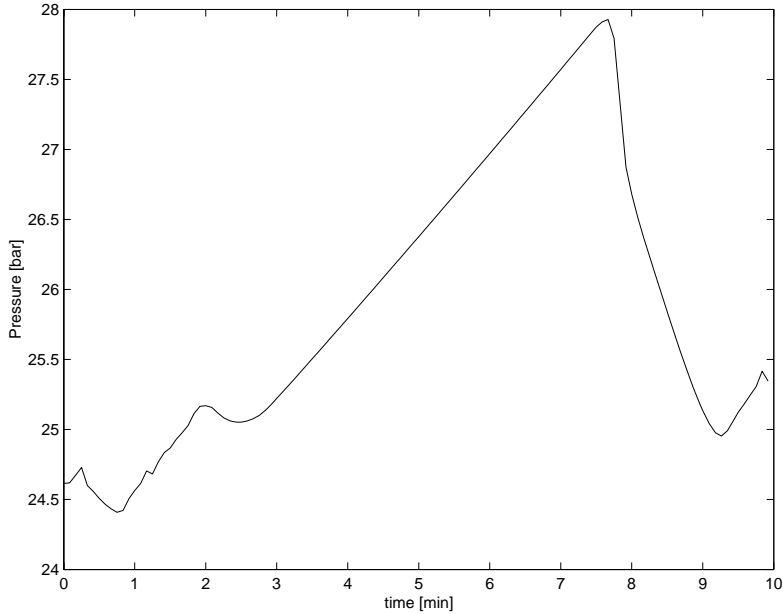
Figure 5: Pressure (at axial distance x=300m) in the horizontal pipe section through a slug cycle.

7 Stability Properties

The bifurcation diagram for the system with the valve opening as independent variable is shown in figure 6. The dotted line indicates the stationary points of the system, to the left of the bifurcation point (marked A) these are stable, to the right they are unstable. The solid lines represent the maximum and minimum pressures of the open loop stable limit cycle. For valve openings between 0.15 to 0.3, the limit cycle is multiperiodic as shown in figure 7. The intermediate pressure levels are not shown in figure 6. The reason for the seemingly strange behavior of the open loop pressures is that it is the intermediate pressure peaks that sustain as the valve opening is increased,

This chart in figure 6 is consistent with a Hopf bifurcation in the system; upon increasing the value of the independent variable, the system goes from a stable state through a bifurcation point into limit cycles with increasing amplitude.

The real part of the "worst" pole (furthest into the right half plane) of the system evaluated at the stationary points is plotted as function of valve position in figure 8. As expected, the onset of instability coincides with the bifurcation point in figure 6.

The root-locus plot for the unstable poles are given in figure 9. This plot shows that the instability occurs as a result a pair of complex conjugate poles moving into the right half plane, consistent with a Hopf bifurcation.
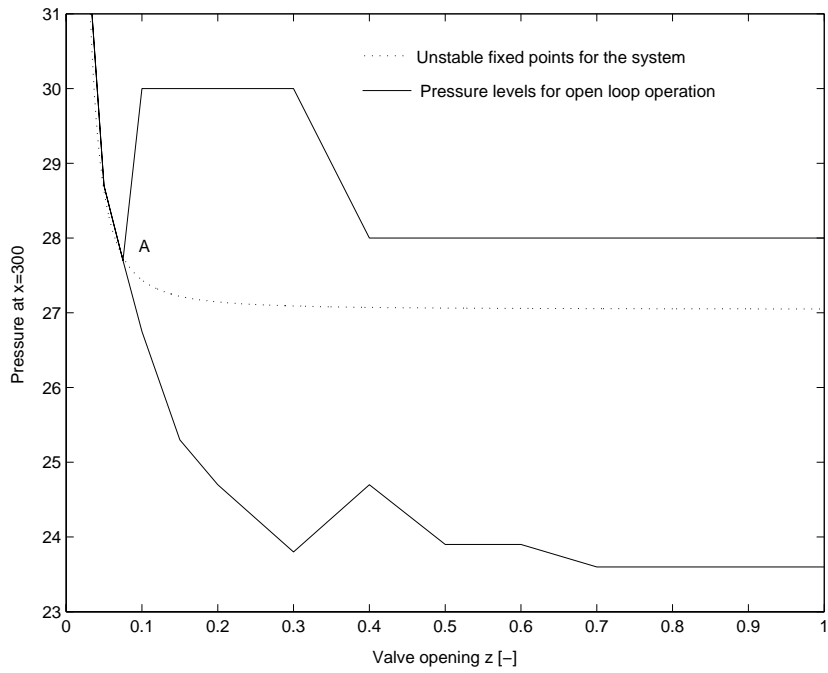
Figure 6: Steady state pressure at x=300m as function of valve opening
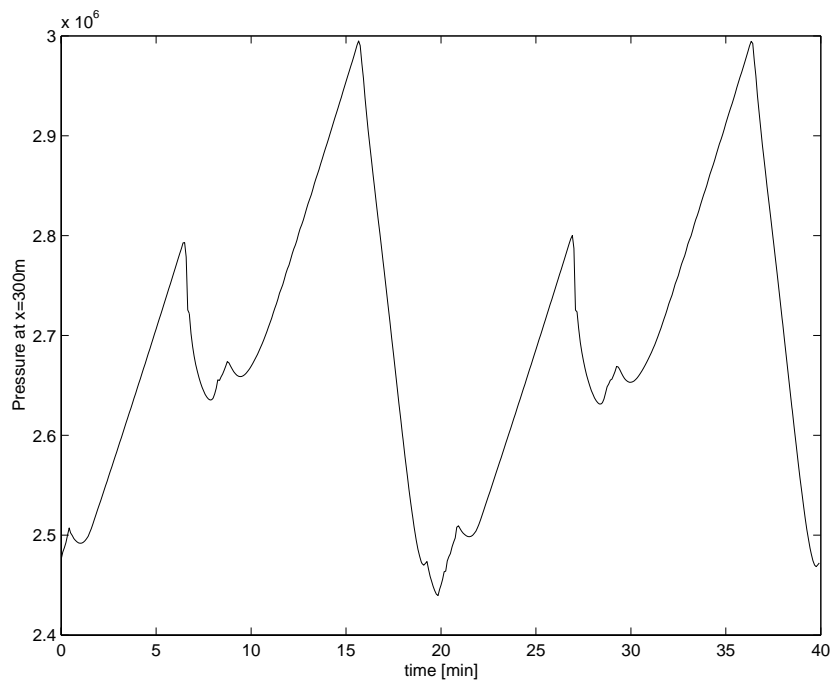
Figure 7: Pressure trend with valve opening 0.2
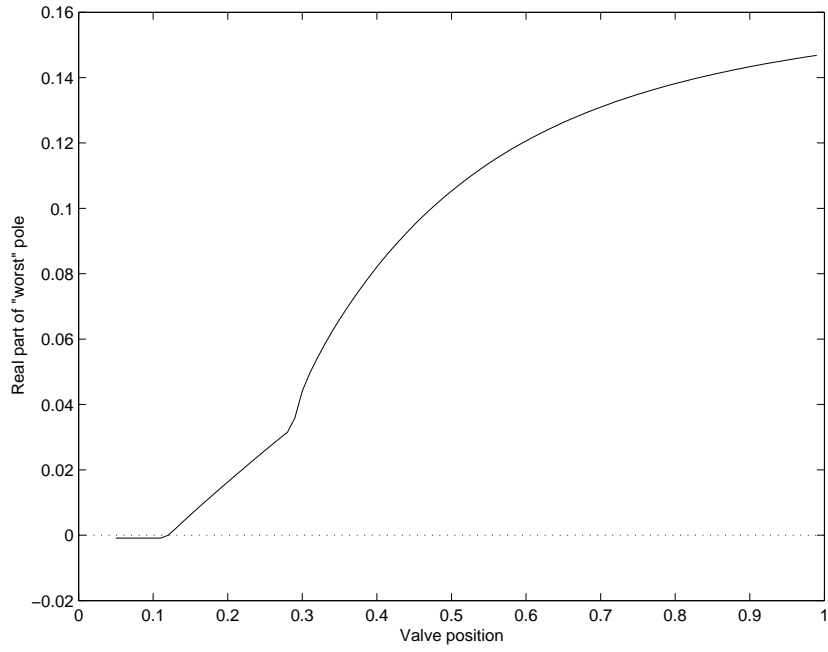
Figure 8: Real part of the "worst" pole as function of valve position
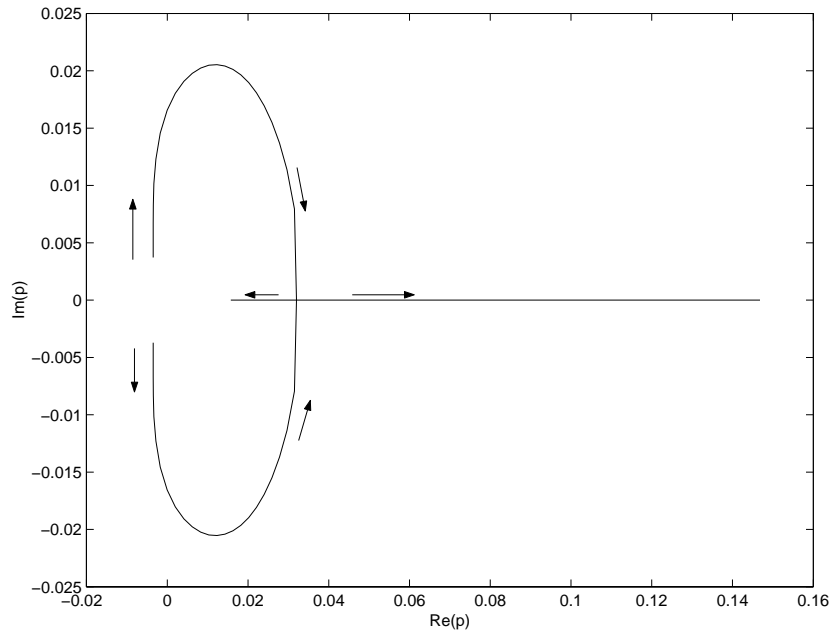
Figure 9: Root-locus plot for the unstable poles
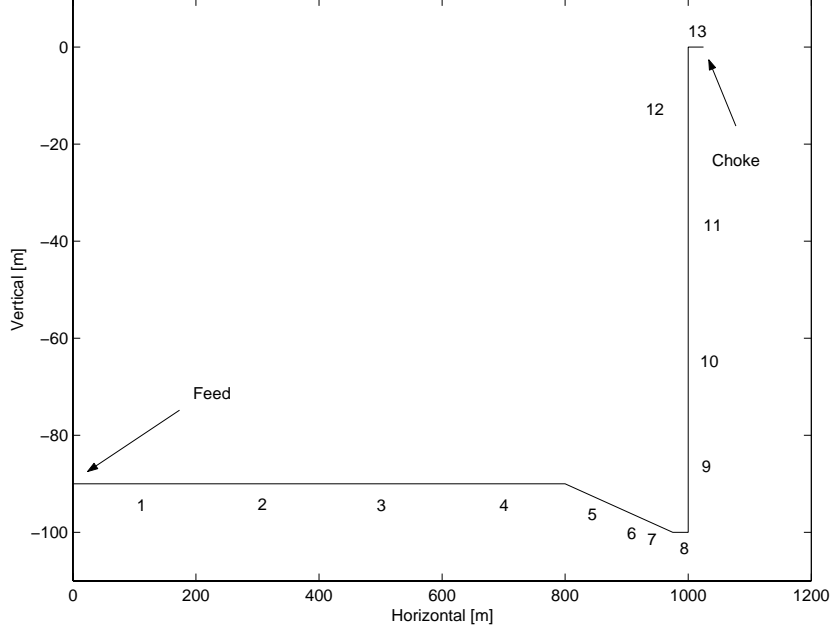
Figure 10: Possible locations for pressure sensors

The gradient dp/dz at the stationary points in figure 6 approaches zero with increasing valve opening. This implies that the process gain from input z to output P approaches zero with increasing valve opening, at the same time as the "worst" pole moves further into the right half plane. As a consequence, it is practically impossible to stabilize the system with large valve openings, since at these operating points, we lack the input power to influence the system sufficiently. We will further support this conclusion below, when discussing controllability. However, the flattening nature of the stationary points also implies that the losses in terms of increasing pressure drop when operating with relatively low valve openings are small.

8 Controllability analysis

In order to cover a wide area of operation, we will in this section consider two operating points: an "easy" one with valve opening 0.15 and a "difficult" one with valve opening 0.4. When considering measurements, 13 different locations are included (coincident with grid resolution). These will be referred to as location 1 through 13, the actual position of these possible sensors are given in figure 10.

The pole vectors gives valuable information on the optimal location of the pressure sensor. The dominant direction of the pole vector is an indication of the best measurement location. The reason for this is that choosing the measurement with the largest element in the pole vector minimizes the lower
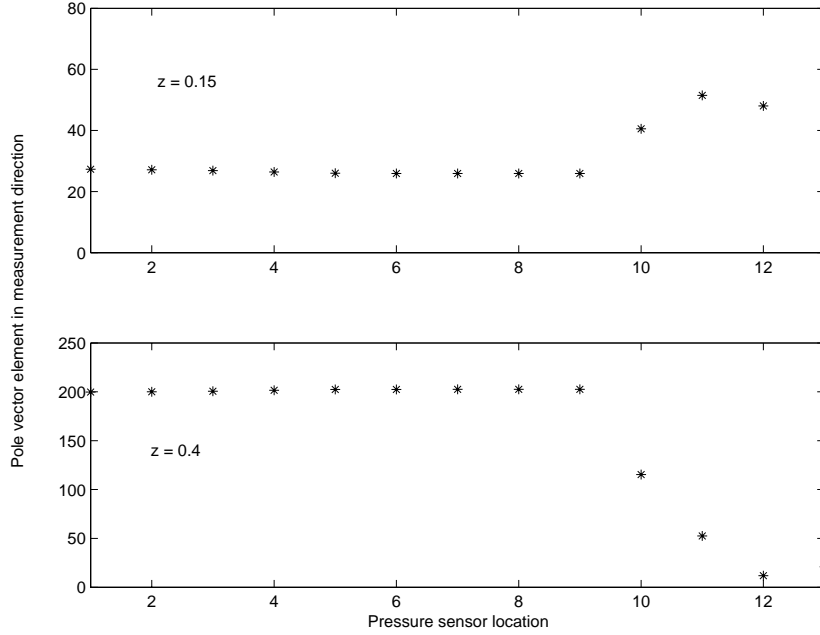
Figure 11: Pole vectors for the operating points z = 0.15 and 0.4

bound on both the $\mathcal{H}_2$ and $\mathcal{H}_\infty$ norm of the transfer function KS from measurement noise to input. More information about pole vectors can be found in Havre (1998) and Havre and Skogestad (1998).

The pole vectors of the unstable poles for the two operating points are illustrated in figure 11. For the first operating point, the pole vector indicates that the pressure sensor should be located high up in the riser section. The second case indicates that the pressure sensor should be located in the horizontal or declining section. To understand why the results are so different for the two operating points, we must consider process gain and right half plane (RHP) zeros.

The RHP zeros limit the achievable bandwidth of the control system. As can be seen from figure 12, with the pressure sensor located close to the top of the riser, the RHP zeros lie close to the imaginary axis. With the pressure sensor located in the declining or horizontal section, RHP zeros will not limit performance. To be able to stabilize the system, the RHP zero must lie to the right of the unstable pole in the complex plane. This is not the case with z = 0.4 and the pressure sensor high up in the riser. For z=0.15, stabilization with some of these measurements is possible, but the pole and the zero is still close, and model uncertainty may well lead to problems even at this operating point.

As previously mentioned, the process gain drops with increasing valve opening. The process gain with the pressure sensor located in the riser is high for low valve openings, but drop significantly with increasing valve opening.

13
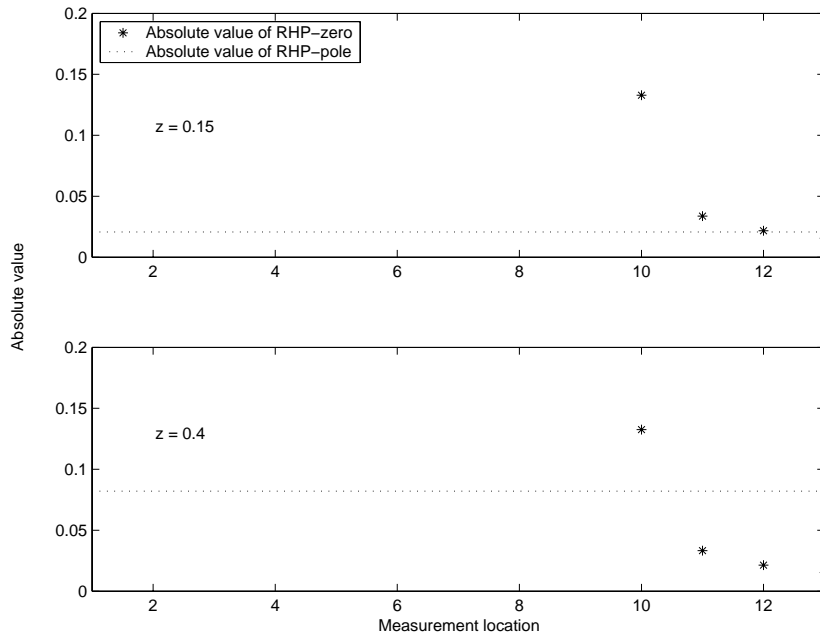
Figure 12: RHP zeros for different measurements, z = 0.15 and 0.4

With the pressure sensor in the declining or horizontal section, the gain still drops with increasing valve opening, but less steeply.

The RHP-zeros and process gain explains why pole direction analysis gives significantly different results for low and high valve openings. Even though it seems that placing the pressure sensor in the riser seems promising when considering the operating point with z=0.15, the RHP-zero analysis shows that this is infeasible for more "aggressive" operation. From this analysis, it is recommended to place the pressure sensor in the lower part of the system. We will in the next section use a pressure measurement placed in the horizontal part at the bottom of the system(point 9 in figure 10).

9   Simple closed loop example

Stabilizing the system consists of two tasks. First the limit cycle has to be broken and the system brought to the desired operating point. Then the system has to be stabilized and kept in this (unstable) state. One can visualize this as a controlling device consisting of two parts, one designed to break the limit cycle and one designed to stabilize the system.

measurement→ ⏍Limit cycle breaker⏎ →⏍Stabilizing controller⏎→ output

Note that the term controlling device does not necessarily imply that both tasks has to be done by an automatic controller.

14
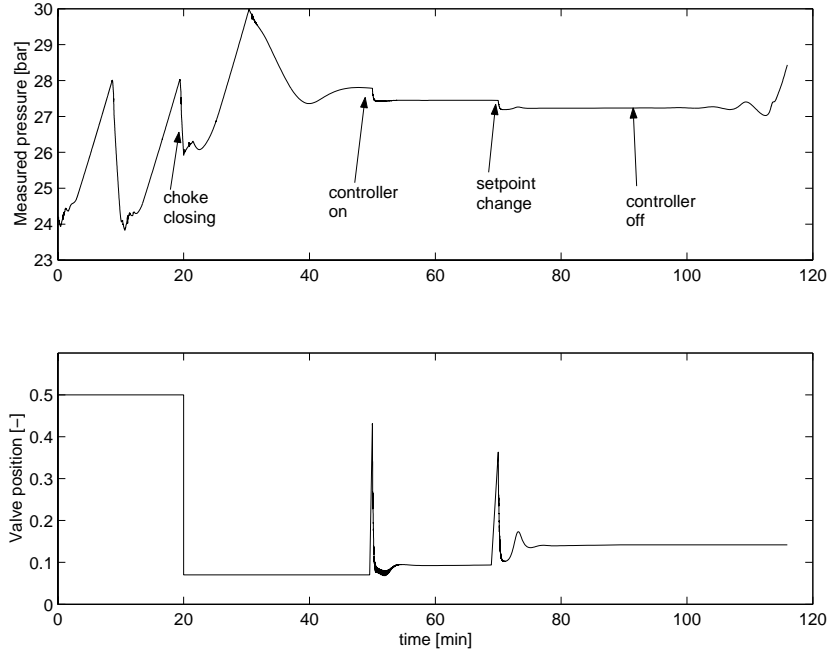
Figure 13: Simple closed loop example

Due to the highly nonlinear nature of the limit cycle behavior, the first part of the controller designed to achieve both tasks probably would need nonlinear elements. An alternative is to manually decrease the valve opening, until the system is stable. Then the control loop is closed and the set point is gradually increased until the desired operating point is reached. In this case, the operator would be the "Limit cycle breaker".

In figure 13, the system is initially operating with a valve opening of 0.5. The choke valve is then closed manually to an opening of 0.07, making the system stable. Using a simple PI-controller, the control loop is then closed, and the set point is gradually decreased, first to 27.46 bar (z = 0.1) then to 27.35 bar (z = 0.15) . This brings the system into the unstable region. Turning the controller off, leaving the valve in the same position, results in instability. This confirms that the steady-state operating point is open-loop unstable

10   Conclusions

In this paper a simple two-phase flow model has been developed. The model captures the main dynamics of severe slugging, and is first order continuous, thus suited for linear analysis and controller design. We have shown that a system exhibiting severe slugging is a Hopf bifurcation with the choke valve position as free variable.

Inside the limit cycle there exists an unstable stationary operating point. The gain of the system approaches zero as the valve opening is increased, at the same time the unstable poles move further into the right half plane. Because of this, stabilizing the system with large valve openings is not practically possible. However, the losses in terms of pressure drop are small even if one operates at quite low valve openings.

The pressure sensor used as measurement for control should be placed in the lower part of the system. With the pressure sensor located in the riser, RHP-zeros close to the imaginary axis limits the bandwidth of the control system, making stabilization of the system difficult.

Stabilizing the system consists of two tasks. First the limit cycle has to be broken and the system brought to the desired operating point. Nonlinear aspects will probably be important for achieving this. Then the system has to be stabilized and kept in this (unstable) state. A linear controller should be sufficient for this.

11 Acknowledgment

References

Baker, D. (1954), 'Simultanous flow of oil and gas', *Oil and Gas J.* **53**, 183–195.

Bewley, T. (2000), 'Flow control: new challenges for a new renaissance', *Progress in Aerospace Sciences* **37**, 21–58.

Havre, K. (1998), Studies on Controllability analysis and control structure design, PhD thesis, Norwegian University of Science and Technology.

Havre, K. and Skogestad, S. (1998), Selection of variables for regulatory control using pole vectors, *in* 'Proc. IFAC symposium DYCOPS-5, Corfu, Greece', pp. 614–619.

Havre, K., Stornes, K. and Stray, H. (2000), 'Taming slug flow in pipelines', *ABB review* **4**, 55–63.

Hedne, P. and Linga, H. (1990), 'Supression of terrein slugging with automatic and manual riser choking', *Advances in Gas-Liquid Flows* pp. 453–469.

Henriot, V., Courbot, A., Heintze, E. and Moyeux, L. (1999), 'Simulation of process to control severe slugging: Application to the dunbar pipeline', SPE Annual Conferance and Exibiton in Huston,Texas. SPE 56461.

Patankar, S. (1980), *Numerical Heat Transfer and Fluid Flow*, Series in Computational Methods in Mechanics and Thermal Sciences, Hemisphere Publishing Company.

Sachdeva, R., Schmidt, Z., Brill, J. and Blais, R. (1986), 'Two phase flow through chokes'. SPE 15657.

Sarica, C. and Tengesdal, J. (2000), 'A new teqnique to eliminating severe slugging in pipeline/riser systems', SPE Annual Technical Conference and Exibition, Dallas, Texas. SPE 63185.

Schmidt, Z., Brill, J. and Briggs, H. (1979), 'Experimental study of severe slugging in a two-phase pipeline-riser system'. SPE 8306.

Taitel, Y. (1986), 'Stability of severe slugging', *Int. J. Multiphase Flow* **12**(2), 203–217.

Appendix 1 : Modeling details

The partial differential equations describing the system is described in chapter 5.

$$\frac{\partial}{\partial t}\left(\alpha_L \rho_L\right) + \frac{1}{A}\frac{\partial}{\partial x}\left(\alpha_L \rho_L u_L A\right) = 0$$

$$\frac{\partial}{\partial t}\left(\alpha_G \rho_G\right) + \frac{1}{A}\frac{\partial}{\partial x}\left(\alpha_G \rho_G u_G A\right) = 0$$

$$\frac{\partial}{\partial t}\left(\alpha_L \rho_L u_L\right) + \frac{1}{A}\frac{\partial}{\partial x}\left(\alpha_L \rho_L u_L^2 A\right) = -\frac{\alpha_L}{A}\frac{\partial}{\partial x}\left(\alpha_L A\right) + \alpha_L \rho_L g_x - \frac{S_{Lw}}{A}\tau_{Lw} + \frac{S_i}{A}\tau_i$$

$$\frac{\partial}{\partial t}\left(\alpha_G \rho_G u_G\right) + \frac{1}{A}\frac{\partial}{\partial x}\left(\alpha_G \rho_G u_G^2 A\right) = -\frac{\alpha_G}{A}\frac{\partial}{\partial x}\left(\alpha_G A\right) + \alpha_G \rho_G g_x - \frac{S_{Gw}}{A}\tau_{Gw} + \frac{S_i}{A}\tau_i$$

The algebraic relations used for friction correlations are:

$$\tau_{kw} = f_w \rho_k \frac{u_k^2}{2}$$

$$\tau_i = f_i \rho_g \frac{(u_G - u_L)^2}{2}$$

$$f_w = \max\left(\frac{64}{Re_k}, 0.005\left(1 + \left(\frac{2 * 10^4 \epsilon}{D_{hk}} + \frac{10^6}{Re_k}\right)^{1/3}\right)\right)$$

$$f_i = 0.02\frac{1 + 75\alpha_L}{4}$$

The wetted perimeters are implicit in phase fraction, and is approximated by polynomials:

$$S_i(\text{stratified}) = \left(\alpha_L^2 - \alpha_L\right)(-4D)$$

$$S_i(\text{annular}) = \pi D\sqrt{\alpha_G}$$

$$S_i(\text{bubble}) = \frac{\pi \alpha_G D^2}{Db}$$

$$S_{kw} = \pi \alpha_k D$$

The notation used for phases k = L and G are:

18

Symbol	Description	Unit
α_k	Volume fraction	
ρ_k	Density	kg/m^3
x	Axial distance	m
u_k	Local phase velocity	m/s
A	Pipe cross-section	m^2
g_x	Gravity vector in pipe direction	m/s^2
S_{kw}	Wetted perimeter between phase k and pipe wall	m
S_{ki}	Wetted perimeter between the phases	m
τ_{kw}	Wall friction	Nm^2
τ_{ki}	Interphase friction	Nm^2
ϵ	Wall roughness	m
D_{hk}	Hydraulic diameter for phase k	m
Re_k	Reynolds number	-
Db	Bubble diameter	m